Production of Photocurrent due to Intermediate-to-Conduction-Band Transitions: A Demonstration of a Key Operating Principle of the Intermediate-Band Solar Cell

A. Martí,[1] E. Antolín,[1] C. R. Stanley,[2] C. D. Farmer,[2] N. López,[1] P. Díaz,[2] E. Cánovas,[1] P. G. Linares,[1] and A. Luque[1]

[1]*Instituto de Energía Solar, Universidad Politécnica de Madrid, E.T.S.I.Telecomunicación, Ciudad Universitaria s/n Madrid, Madrid 28040, Spain*

[2]*Department of Electronics and Electrical Engineering, University of Glasgow, Glasgow, G12 8QQ, United Kingdom*

(Received 15 August 2006; published 13 December 2006)

We present intermediate-band solar cells manufactured using quantum dot technology that show for the first time the production of photocurrent when two sub-band-gap energy photons are absorbed simultaneously. One photon produces an optical transition from the intermediate-band to the conduction band while the second pumps an electron from the valence band to the intermediate-band. The detection of this two-photon absorption process is essential to verify the principles of operation of the intermediate-band solar cell. The phenomenon is the cornerstone physical principle that ultimately allows the production of photocurrent in a solar cell by below band gap photon absorption, without degradation of its output voltage.

DOI: 10.1103/PhysRevLett.97.247701 PACS numbers: 84.60.Jt, 72.40.+w, 73.50.Pz, 85.60.Dw

The basic principles of operation of the intermediate-band solar cell (IBSC) were originally described by Luque and Martí in 1997 [1]. This novel cell relies on so-called intermediate-band material which is characterized by the existence of a band (the intermediate, IB) located between the conventional conduction and valence bands of a semiconductor [Fig. 1(a)].

The presence of the IB leads to the generation of one net electron-hole pair when two below band gap photons are absorbed. One photon (photon "1") pumps an electron from the valence band (VB) to the IB while a second (photon "2") pumps an electron from the IB to the conduction band (CB). This electron-hole pair adds to those produced conventionally by photons with above band gap energy E_G that excite electrons directly from the VB to the CB (photon "3"). A necessary requirement is that the IB is half-filled with electrons to provide both empty states to receive electrons from the VB and filled states to provide electrons to be supplied to the CB [2].

A further condition for successful operation of the IBSC is that the carrier population in each band is described by its own quasi-Fermi level [Fig. 1(b)]. This follows from the fact that the bands are isolated from each other by a zero density of states, and hence, the lifetimes associated with carrier recombination from one band to another are expected to be much longer than carrier relaxation times within each band. These quasi-Fermi levels are E_{FC}, E_{FI}, and E_{FV} for the CB, IB, and VB, respectively. The output voltage, V, of the cell is related to the quasi-Fermi levels by $eV = E_{FC} - E_{FV}$ where e is the electron charge. To effectively obtain this split, the material containing the intermediate-band has to be sandwiched between two single gap semiconductors, one p-type and the other n-type. The current-voltage characteristic of the device is modeled by solving the electron and hole continuity equations, as described in detail in Ref. [2,3].

It can be demonstrated rigorously [1,2] that the output voltage is limited by the total band gap E_G and not by the lower of the band gaps E_L or E_H, as shown in Fig. 1(b). In consequence, the photocurrent gain achieved from the absorption of below band gap photons can occur without photo-voltage degradation. Within this framework, a limiting efficiency of 63.2% has been predicted for the IBSC, compared to 40.7% for conventional single gap solar cells and 55.4% for 2-junction tandem solar cells. These limits have been extended by Green *et al.* [4] to 86.8% (the same as the absolute limit for photovoltaic energy conversion [5]) for the case in which multiple bands exist within the semiconductor band gap. Essentially, these efficiency figures are derived using the approximations in the Shockley and Queisser detailed balance [6] calculations which imply, in particular, that recombination to and from the IB takes place in the radiative limit. Luque *et al.* [7] have

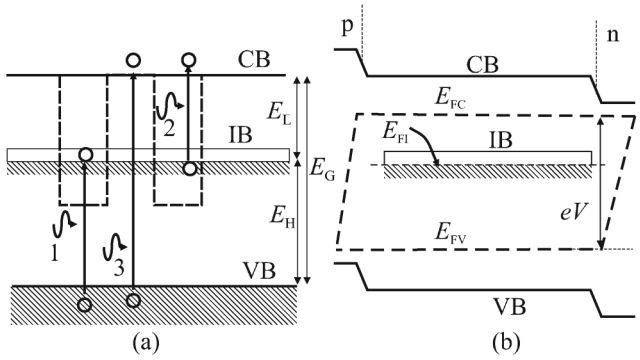

FIG. 1. Basic operation of an intermediate-band solar cell (a) structure of the intermediate-band material showing the absorption processes involved [1]; (b) intermediate-band material sandwiched between p and n type semiconductors showing the relation between voltage and quasi-Fermi level separation [2].

discussed mechanisms that can prevent the IB from becoming a collection of non-radiative recombination centers which would be detrimental instead of beneficial for the IBSC performance. They have also proposed how to avoid them based on increasing the density of the centers that introduce the intermediate levels beyond the Mott transition.

Concerning the existence of bulk intermediate-band materials, Yu *et al.*. have found experimental evidence of multiple band formation in diluted II-VI oxide semiconductors [8] and GaNAsP quaternary alloys [9]. Several authors have predicted the formation of an IB band in $CuGaS_2$ with 25% of Ga atoms substituted by Ti [10], and in $M_xGa_{1-x}P$ [11–13] where M is either Ti or Cr.

It should be noted that the below band gap energy photons are capable of pumping electrons from both the VB to the IB and the IB to the CB. At room temperature, however, another mechanism is also possible, namely, photon pumping of electrons from the VB to the IB with subsequent thermal escape from the IB to the CB, removing the need for a second photon to promote the IB to CB transition. In this circumstance, it is impossible for the output voltage to exceed the band gap E_H without violating the second law of thermodynamics [14,15]. Therefore, of the transitions described above and illustrated in Fig. 1(a), those corresponding to the absorption of photons causing transitions from the IB to the CB are particularly important. The bulk of this Letter focuses on experiments which demonstrate IB-CB absorption and the subsequent production of photocurrent, one of the key fundamental principles that govern the operation of the IBSC.

The IBSCs used in our experiments were processed from InAs/(Al,Ga)As quantum dot (QD) structures grown by molecular beam epitaxy using the Stransky-Krastanov growth mode [16]. The IB arises from the confinement of electrons in the conduction band [17], as shown in Fig. 1(a). Details of the internal structure of the devices used in the experiments are shown in Fig. 2. A discussion justifying this structure will be postponed until the experimental results have been presented.

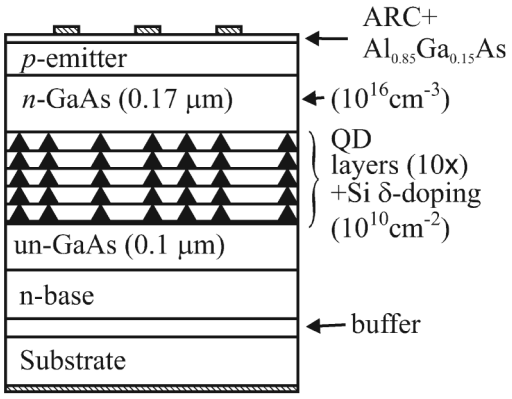

FIG. 2. Structure of the quantum dot intermediate-band solar cells used in the experiments.

The In flux was calibrated by reflection high energy electron diffraction (RHEED) intensity oscillations from an InAs wafer and set to a growth rate of 0.032 monolayers per second (ML/s). A stack of 10 QD and capping layers was grown consisting of 3.2 ML of InAs deposited at ~460 °C followed 5 nm of un-GaAs, Si δ-doping with an areal density of 1×10^{10} cm^{-2} to match the QD density, and a further 3.5 nm of un-GaAs to complete the capping of the dots. At this point in the growth of the stack, the substrate temperature was raised to 580 °C and held there for 10 minutes to smooth the surface of the GaAs cap [Ref. [18,19]]. The wafer temperature was then lowered back to ~460 °C and the next period of the QD stack grown. The optical properties of the stack were checked by measuring the spontaneous emission (EL) from the devices when forward biased as LEDs. The EL spectrum at 20 K showed two distinct peaks at wavelengths of ~1110 nm and 1180 nm, which merged to emit virtually as a single peak in the range ~1180–1300 nm at 300 K.

In the experiments carried out in the past by our groups [20–23], the quantum dot intermediate-band solar cells (QD-IBSC) have failed to provide straightforward proof of the IBSC principles. However, the preliminary experiments have shown that QD-IBSCs illuminated with below band gap energy photons (photons with energy above E_H but below E_G), do produce photocurrent. This is still the case in the new batch of samples presented in this work as shown by curve 1 in Fig. 3.

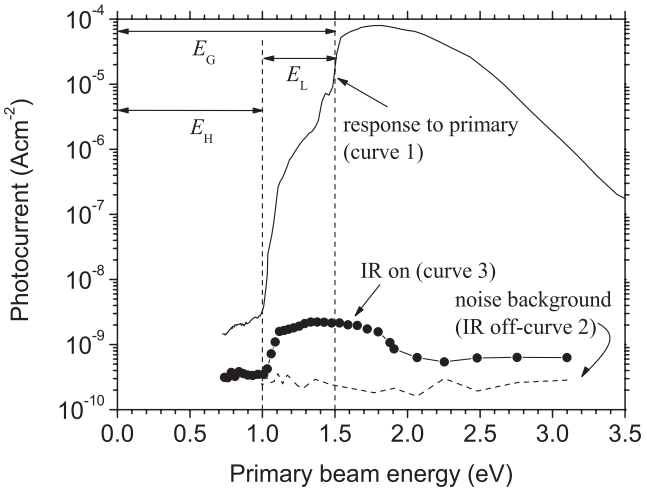

FIG. 3. Photocurrent produced in the QD-IBSC samples as a function of the energy of the photons of the primary light source. Curve 1 (response to primary) represents the photocurrent produced when pumping with the chopped primary source only ($V = -1.5$ V, $T = 4.2$ K). Curve 2 (noise background) is the photocurrent measured when the IR source is off while the chopper, located in front the of the IR source, is kept spinning ($V = 0$ V, $T = 36$ K). Curve 3 (IR on) is the photo-generated current when the IR source is turned on and chopped ($V = 0$ V, $T = 36$ K). Device junction area is 4 mm [2].

Proof for the crucial, optically induced IB-CB transition has been obtained from the experiment outlined in Fig. 4. The QD-IBSC sample is located inside a closed cycle He cryostat in which two optical windows have been opened. Experiments presented here are carried out at 36 K. Light from a monochromator diffracting the white light from a halogen lamp is introduced through one of the windows. This light (primary light source) is not chopped and is filtered by an appropriate set of filters to remove secondary wavelengths from the experiment. Its basic role is to supply photons for continuous pumping of electrons from the VB to the IB. Light from an infrared light source, filtered with a 350 μm thick GaSb wafer and chopped at 377 Hz, is introduced through the second cryostat window. The role of this IR source, together with the GaSb filter, is to illuminate the QD-IBSC with photons of energy below the GaSb bandgap (0.726 eV) so that they only have sufficient energy to pump electrons from the IB to the CB (and not from the VB to the IB or from the VB to the CB). Above 0.726 eV, for example, for photon energies of 0.8 eV, only one among 10^{75} photons will pass through the GaSb filter, assuming an absorption coefficient [24] of 5000 cm^{-1}. This number will be lower for higher photon energies since the absorption coefficient increases rapidly with the photon energy.

The photocurrent produced by the cell is collected through a low noise and low input impedance current-voltage preamplifier that can bias the QD-IBSC at 0 volts (short-circuit). The biasing is checked independently with a voltmeter connected to the sample in a 4-wire Kelvin connection. The output signal voltage from the preamplifier is taken to a lock-in amplifier. The experimental arrangement allows the impact of IB-CB absorption on the overall photocurrent to be distinguished from other current generating processes.

First, the current from the QD-IBSC is measured with the IR source off (but the chopper on) as the monochromator scans and illuminates the sample with an unmodulated stream of photons of different energies. In the absence of IB-CB transitions, this should not produce any ac current in the cell, as is the case experimentally. It provides the noise base line for the measurement and is plotted in Fig. 3 for reference (curve 2). Spurious signals, for example, light from the monochromator that could be reflected from the spinning chopper blades and thus mask the result of the experiment, would be detected. Next, the IR source is switched on while the monochromator scans again. The result of this measurement is also plotted in Fig. 3 (curve 3). A clear ac photocurrent from the QD-IBSC is detected that can only be caused by absorption of photons emanating from the filtered IR source that, being filtered by the GaSb wafer, have only enough energy to pump electrons from the IB to the CB, and not from the VB to the IB. This is an important result in support of the basic operating principles of the IBSC.

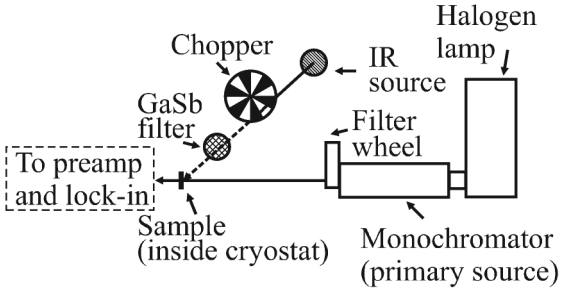

FIG. 4. Description of the experimental setup.

We also include in Fig. 3 (curve 1) the photo-generated current when the IR source is removed from the setup and the chopper is located on the optical branch containing the monochromator. The sub-band gap photocurrent measured under this experimental condition arises from photons with energies in the range $\approx$ 1.0–1.5 eV, i.e., below the band gap E_G but above E_H. These pump electrons from the VB to the IB and subsequently to the CB. Other mechanisms, including a photon of this same energy pumping an electron from the IB to the CB, are also possible. Note that the threshold for the production of photocurrent with both light sources illuminating the QD-IBSC (curve 3) occurs at the energy where the primary source provides photons capable of pumping electrons from the VB to the IB. This reinforces the result of the experiments and rules out the possibilities that (i) IR light is imperfectly filtered by the GaSb or (ii) spurious light comes into the QD-IBSC. Moreover, the photocurrent signal is not altered at the energy threshold E_G, where direct pumping from the VB to the CB is possible, confirming that these photons are being used to pump electrons from the VB to the IB. In addition, the photocurrent signal decays for photon energies $\geq$ 1.9 eV since the 0.9 μm thick GaAs emitter of the cell is absorbing strongly and the primary light is unable to penetrate to the region containing the QDs.

It is important to note that the influence of the IR source has been detected on the short-circuit conditions, i.e., with zero volts applied bias across the device. The photovoltaic mode for the detection of the IR radiation is in contrast to other IR detectors, also using low dimensional structures such as quantum wells, where detection of light is based on an increment of photoconductivity [25] under electrical bias.

We now return to the details of the structure outlined in Fig. 2. In the first place, quantum dots and no other low dimensional structures like quantum wells or wires are preferred because they isolate the IB from the CB with a zero density of states. The inclusion of the delta doping layers, with an intended areal doping density (10^{10} cm^{-2}) equal to the QD density, is necessary to half-fill the IB with electrons [26]. This is particularly important at low temperatures since, otherwise, the IB would be completely emptied of electrons and the pumping of electrons from

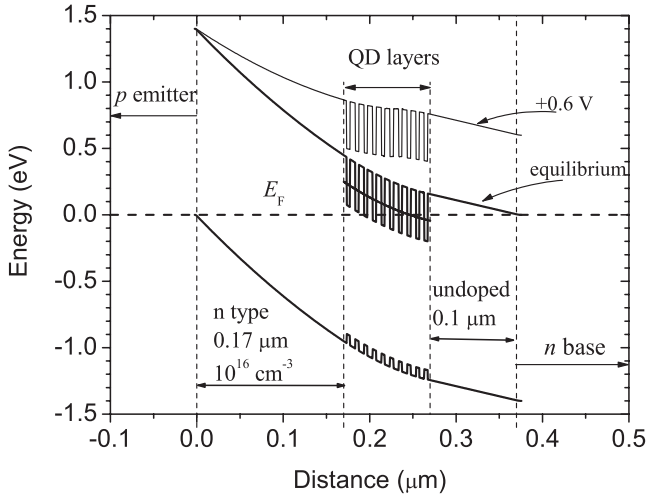

FIG. 5. Simplified band gap diagram of the QD-IBSC in equilibrium and under 0.6 V forward bias.

the IB to the CB would have to rely exclusively in the capacity of the primary beam to populate the IB.

The 10^{16} cm^{-3} n-type layer of the structure is intended to be partially depleted so that the QDs are located in a flat-band potential region. This will ensure that half-filling of the IB extends through a large number of QD layers. Following a conservative design, the doping level and thickness of this layer (as well as the undoped layer below the QDs) were chosen [26] to place the QD layers into flat-band conditions at the expected forward bias with the cell approaching its maximum power point (Fig. 5).

The thin undoped layer is also designed to sustain part of the junction electric field to establish a flat-band potential region for the QDs. It also prevents tunneling from the n-emitter into the IB.

In conclusion, by using quantum dot technology to implement the IBSC, we have shown that it is possible to pump electrons from the IB to the CB and produce photocurrent. This is one of the fundamental physical principles on which the operation of the IBSC is based and opens the way for future photovoltaic devices in which the IB can contribute to photocurrent enhancement without voltage degradation. The aim now is to enhance the optical absorption provided by the QDs while preserving the material quality, to increase the current generated by sub-band gap photons.

This work has been supported by the European Commission within the Project FULLSPECTUM (No. SES6-CT-2003-502620) and the Projects NUMANCIA (No. S-0505/ENE/000310) funded by the Comunidad de Madrid and GENESIS-FV (No. CSD2006-00004) funded by the Spanish Consolider National Programme.

[1] A. Luque and A. Martí, Phys. Rev. Lett. **78**, 5014 (1997).
[2] A. Luque and A. Martí, Progress in Photovoltaics: Research and Applications **9**, 73 (2001).
[3] A. Martí, L. Cuadra, and A. Luque, IEEE Trans. Electron Devices **49**, 1632 (2002).
[4] A. M. Green, Progress in Photovoltaics: Research and Applications **9**, 137 (2001).
[5] A. De Vos and H. Pauwels, Applied Physics (Berlin) **25**, 119 (1981).
[6] W. Shockley and H. J. Queisser, J. Appl. Phys. **32**, 510 (1961).
[7] A. Luque, A. Martí, and E. Antolín *et al.*, Physica B (Amsterdam) **382**, 320 (2006).
[8] K. M. Yu, W. Walukiewicz, and J. Wu *et al.*, Phys. Rev. Lett. **91**, 246403 (2003).
[9] K. M. Yu, W. Walukiewicz, and J. W. Ager *et al.*, Appl. Phys. Lett. **88**, 092110 (2006).
[10] P. Palacios, K. Sánchez, and J. C. Conesa *et al.*, Phys. Status Solidi A **203**, 1395 (2006).
[11] P. Palacios, J. J. Fernandez, and K. Sanchez *et al.*, Phys. Rev. B **73**, 085206 (2006).
[12] C. Tablero and P. Wahnon, Appl. Phys. Lett. **82**, 151 (2003).
[13] C. Tablero, Solid State Commun. **133**, 97 (2005).
[14] A. Luque, A. Martí, and L. Cuadra, IEEE Trans. Electron Devices **48**, 2118 (2001).
[15] A. Luque, A. Martí, and L. Cuadra, Physica E (Amsterdam) **14**, 107 (2002).
[16] M. Sugawara, *Self-assembled* InGaAs/GaAs *Quantum Dots* (Academic Press, New York, 1999).
[17] A. Martí, L. Cuadra, and A. Luque, in *Proc. of the 28th IEEE Photovoltaics Specialists Conference* (IEEE, New York, 2000).
[18] E. C. Le Ru, A. J. Bennett, C. Roberts, R. Murray, J. Appl. Phys. **91**, 1365 (2002).
[19] E. C. L. Ru, P. Howe, and T. S. Jones *et al.*, Phys. Rev. B **67**, 165303 (2003).
[20] A. Luque, A. Martí, and C. Stanley *et al.*, J. Appl. Phys. **96**, 903 (2004).
[21] A. Luque, A. Martí, and N. López *et al.*, Appl. Phys. Lett. **87**, 083505(2005).
[22] A. Martí, N. López, and E. Antolín *et al.*, Thin Solid Films **511–512**, 638 (2006).
[23] A. Luque, A. Martí, and N. López *et al.*, J. Appl. Phys. **99**, 094503 (2006).
[24] A. Y. Vul, in *Handbook Series on Semiconductor Parameters*, edited by M. Levinshtein, S. Rumyantsev, and M. Shur (World Scientific, Singapure, 1996), Vol. 1, Chap. 5.
[25] J. P. Loehr and M. O. Manasreh, *Semiconductor Quantum Wells and Superlattices for Long-Wavelength Infrared Detectors* (Artech House, Boston, 1993).
[26] A. Martí, L. Cuadra, and A. Luque, IEEE Trans. Electron Devices **48**, 2394 (2001).